Isomeric cross-section ratio for the formation of $^{58}Co^{m,g}$ in neutron, proton, deuteron, and alpha-particle induced reactions in the energy region up to 25 MeV

S. Sudár[1,2] and S. M. Qaim[1]
[1]*Institut für Nuklearchemie, Forschungszentrum Jülich GmbH, D-52425 Jülich, Germany*
[2]*Institute of Experimental Physics, Kossuth University, H-4001 Debrecen, Hungary*
(Received 17 November 1995)

Excitation functions were determined for $^{58}Fe(p,n)^{58}Co^{m}$, $^{nat}Fe(d,xn)^{58}Co^{m}$, $^{55}Mn(\alpha,n)^{58}Co^{m}$, and $^{59}Co(n,2n)^{58}Co^{m}$ reactions from the respective thresholds to 14.12 MeV in work with protons, 12.97 MeV with deuterons, 13 MeV with neutrons, and 25.52 MeV with alpha particles. The radioactivity of the activation product $^{58}Co^{m}(T_{1/2}=9.15$ h) was determined by high resolution γ-ray and x-ray spectrometry. Using the present σ_m results and the $(\sigma_m+\sigma_g)$ data reported earlier, the isomeric cross-section ratio $\sigma_m/(\sigma_m+\sigma_g)$ was determined for each reaction. Statistical model calculations taking into account the precompound effects were performed for the above-mentioned four reactions as well as for the $^{58}Ni(n,p)^{58}Co^{m,g}$ process. A consistent set of model parameters was used. The isomeric cross-section ratio for the pair $^{58}Co^{m,g}$ strongly depends on the level scheme and branching ratios of the known levels of ^{58}Co. Different reactions produced different angular momentum distributions of the compound nucleus, resulting in different isomeric cross-section ratio at the same excitation of the compound nucleus. The ratio was found to be relatively high for target nuclei with high spin values. [S0556-2813(96)01506-3]

PACS number(s): 25.40.−h, 24.60.Dr, 25.45.−z, 25.55.−e

I. INTRODUCTION

Studies of excitation functions of nuclear reactions are of considerable significance for testing nuclear models. Furthermore, isomeric cross-section ratios are of fundamental interest for studying the effect of nuclear spin. We chose to investigate the isomeric pair $^{58}Co^{m,g}$, a simplified level scheme of which (cf. Ref. [1]) is given in Fig. 1. The separation energy between the two isomeric levels is only 24.9 keV but the spins differ considerably. Both the states can be populated via seven nuclear processes (cf. Fig. 1), viz. $^{58}Ni(n,p)$, $^{59}Co(n,2n)$, $^{59}Co(p,pn)$, $^{58}Fe(p,n)$, $^{57}Fe(d,n)$, $^{55}Mn(\alpha,n)$, and $^{61}Ni(p,\alpha)$. The total cross section for the formation of the isomeric pair $(\sigma_m+\sigma_g)$ has been measured in detail (cf. Refs. [2–5]) and almost all the excitation functions can be reproduced relatively well by the statistical model (cf. Refs. [3–5]), provided the optical model and level-density parameters are properly chosen. Only in the case of (d,n) process, a reduction factor was needed [4] to take account of the direct breakup contribution.

The present work concentrates primarily on the formation of the isomeric state $^{58}Co^{m}(T_{1/2}=9.15$ h), which is experimentally somewhat difficult to measure. Some data on the $^{59}Co(n,2n)$ and $^{59}Co(p,pn)$ reactions were available in the literature (cf. Refs. [2,6]), and we reported results on the $^{61}Ni(p,\alpha)$ and $^{58}Ni(n,p)$ reactions earlier [3,7]. Now we describe investigations on the other four processes. As suggested in a recent review article [8], these investigations should possibly shed some light on the effect of reaction channels on the isomeric cross-section ratio.

It is known that cross sections for the formation of isomeric states are more difficult to predict than those for the total reaction channels. One of the major goals of this work was therefore to test the applicability of nuclear model calculations to the prediction of isomer ratios over an energy range up to 25 MeV.

II. EXPERIMENT

Cross sections were measured via the activation technique, commonly used both at Jülich and Debrecen. This technique is ideally suited for studying the formation of low-

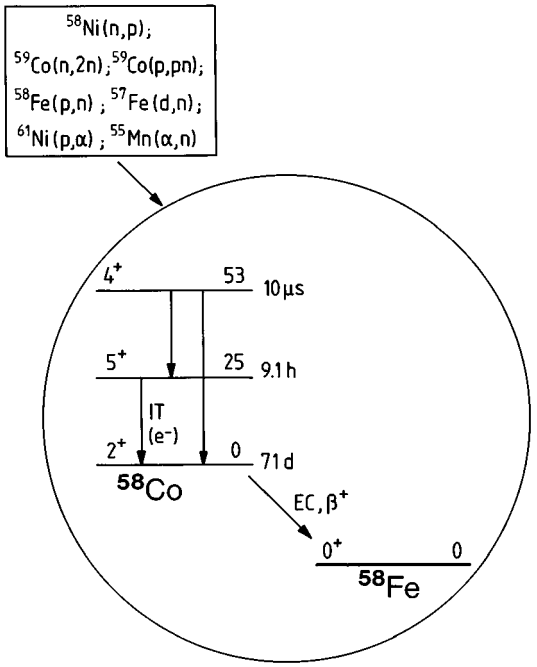

FIG. 1. Simplified representation of formation and decay of the isomeric pair $^{58}Co^{m,g}$. The nuclear level energies are in keV.

lying closely spaced levels, provided their lifetimes are not too short. Some of the features of the technique relevant to the present work are described below.

A. Charged particle irradiations, mean particle energies and beam intensities

For investigations on the ^{55}Mn$(\alpha,n)^{58}$Co^m, ^{58}Fe$(p,n)^{58}$Co^m, and ^{57}Fe$(d,n)^{58}$Co^m reactions the well-known stacked-foil technique was used. The compositions of the stacks and the irradiation details have been described earlier [4]. The methods of calculation of the mean particle energy and beam intensity (i.e., incident particle flux) effective at each foil were exactly the same as in Ref. [4].

B. Neutron irradiations, energies and flux densities

Investigations on the ^{59}Co$(n,2n)^{58}$Co^m reaction were performed in the energy range 11–13 MeV (the data for the total $(n,2n)$ process are known well [2]). Quasi-monoenergetic neutrons were produced via the ^{2}H$(d,n)^3$He reaction on a deuterium gas target (cf. Refs. [9,10]) at the variable energy compact cyclotron CV28 at Jülich. The sample consisted of a Co foil (2.0 cm $\phi\times$0.15 mm) of 99.9% pure metal. It was sandwiched between two Al foils (each 2.0 cm $\phi\times$0.15 mm) and placed at a distance of 1 cm from the end of the gas target in 0° direction to the deuteron beam for the irradiation. At each deuteron energy two irradiations were performed. The typical irradiation time was 30 min. The mean neutron energy for each sample was calculated using a Monte Carlo program NEUT (cf. Ref. [11]) and the mean neutron flux density was determined via the monitor reaction ^{27}Al$(n,\alpha)^{24}$Na (cf. Ref. [12]).

C. Measurement of radioactivity

The radioactivity of each monitor reaction product (cf. Refs. [4,10]) was determined via standard HPGe detector γ-ray spectrometry. In those cases where radioactivity of ^{58}Co^{m+g} was also determined, all the measurements were started after complete decay of ^{58}Co^m to the ground state.

The radioactivity of ^{58}Co^m ($T_{1/2}$=9.15 h) was somewhat difficult to measure. This metastable state decays to the ground state via isomeric transition (IT) which is highly converted; the 24.9 keV γ ray, therefore, cannot be directly detected. There are, on the other hand, two possibilities of determining the initial activity of ^{58}Co^m. In the first method, the activity of the ground state ^{58}Co^g is measured as a function of time via standard γ-ray spectrometry. From an analysis of the growth and decay curve of ^{58}Co^g it is possible to obtain the initial activities of both ^{58}Co^m and ^{58}Co^g. This method was found to be suitable when the activity of ^{58}Co^m was relatively high. In the second method, the activity of ^{58}Co^m is determined via x-ray spectrometry. The radiation encountered consists of $K\alpha$ and $K\beta$ lines of Co as against $K\alpha$ and $K\beta$ lines of Fe in the case of ^{58}Co^g decay (via $EC+\beta^+$ emission). In earlier reports on ^{58}Ni$(n,p)^{58}$Co^m (cf. Ref. [7]) and ^{61}Ni$(p,\alpha)^{58}$Co^m (cf. Ref. [3]) reactions only the x-ray counting method was used. For the former reaction, later the growth and decay method was also attempted [5] and the results were found to be in agreement with the x-ray counting data. In the present work on the four other reactions, we considered both techniques. The growth and decay method led to satisfactory results in the case of ^{55}Mn$(\alpha,n)^{58}$Co^m reaction where the activity of ^{58}Co^m was relatively high. However, for the other three process, viz. ^{59}Co$(n,2n)^{58}$Co^m, ^{58}Fe$(p,n)^{58}$Co^m, and ^{57}Fe$(d,n)^{58}$Co^m, where the amount of ^{58}Co^m was small, the x-ray counting method was found to be superior.

TABLE I. Decay data of the measured reaction products. (Taken from Browne and Firestone [1].)

Radio-isotope	Half-life	Radiation type	γ- or x-ray energy in keV	γ- or x-ray abundance (%)
^{58}Co	70.92d	γ	810.8	99.4
		Fe $K\alpha 2$	6.39	7.7
		Fe $K\alpha 1$	6.40	15.3
		Fe $K\beta 1$	7.06	2.7
^{58}Co ^{m}	9.15h	γ	24.89	$<$0.04
		Co $K\alpha 2$	6.91	7.8
		Co $K\alpha 1$	6.93	15.4
		Co $K\beta$	7.65	2.8

The x-ray spectrometric studies were performed using either a Si(Li) or an intrinsic HPGe (with Be window) detector coupled to an Ortec (Spectrum ACE) 4k MCA Plug-In Card. The other details relevant to the spectrum analysis were the same as for γ-ray spectrometry described earlier [4]. In general only the summed peak area under the $K\alpha$ line was used and an analysis of decay curve was invariably performed.

D. Calculation of cross sections and isomeric cross-section ratios

The count rates were corrected for random pileup losses (using a pulse generator as reference) as well as for γ-ray or x-ray abundance and the efficiency of the detector. Correction for coincidence loss was also taken into account. The most important decay data of the product nuclides ^{58}Co^m and ^{58}Co^g are summarized in Table I. After deriving the initial activities the cross sections were calculated using the usual activation formula. The isomeric cross-section ratio could be determined more simply from the growth and decay curve measurement of the ground-state activity. The x-ray counting method involved a larger error due to the use of two different detectors for measurement of the activities of the ground and isomeric states.

E. Errors

The major sources of errors involved were those associated with the measurement of the beam current (or neutron flux density) and determination of the absolute activities of the products. As discussed in several earlier publications (cf. Refs. [4,10]), the error in the neutron flux density or beam current was adopted as 4–7 %. The efficiencies of the γ- and x-ray detectors were known within an uncertainty of 3–5 %. A few samples were assayed by both the γ-ray growth and decay curve analysis and x-ray counting method, and the

TABLE II. Branching ratio (B) of the 52.8-keV level for different types of transition, calculated using the theoretical conversion coefficient (α).

		Type of transition for the 52.8→24.8 keV deexcitation			
Transition	γ emission	$M1$		$E2$	
	(%)	α	B (%)	α	B (%)
52.8→24.8	29	1.3	11	59.3	77
52.8→0	71	6.5	89	6.5	23

agreement between the measured activities was within 2–3 %, proving that the efficiency calibration procedures were reliable. The errors in the calculation of the absolute activity were: the error of the initial count rate at the end of the irradiation was determined by the least-squares-fitting procedure (see above) and it was about 0.5–25 %; the error in the decay data used was <1% and that in the coincidence losses <0.5%. The error in the target atoms/cm^2 was 0.5–1.5 %. The total error in each cross section was obtained by combining the individual errors in quadrature.

III. NUCLEAR MODEL CALCULATIONS

Cross sections were calculated using the statistical model taking into account the preequilibrium effects. The calculational code STAPRE [13] was applied. The details regarding the calculation of total cross section for each channel have already been described (cf. Ref. [4]). In the present work the emphasis was on the calculation of the isomer cross section. Since such calculations are strongly dependent on the input level scheme of the product nucleus (cf. Refs. [14,15]), we chose those parameters carefully. The energies, spins, parities and branching ratios of the discrete levels were selected from the Nuclear Data Sheets [16]. In the continuum region the level density was calculated as described earlier [4]. Another important consideration in calculating the isomeric cross sections is the spin distribution of the level density (cf. Refs. [3,14]). This was characterized by the ratio of the effective moment of inertia $\Theta_{\rm eff}$ to the rigid-body moment of inertia $\Theta_{\rm rig}$ ($\eta=\Theta_{\rm eff}/\Theta_{\rm rig}$) and the calculations were performed for $\eta=1.0$. The transmission coefficients of photons are also of considerable significance in calculations on isomeric cross sections. They were derived from the gamma-ray strength functions. For the $E1$ radiation the Brink-Axel model with global parameters was applied, while for the $M1$, $E2$, $M2$, $E3$, and $M3$ radiation the Weisskopf model was used.

A weak point in the level scheme of the nuclide ^{58}Co is the level at 52.8 keV. The types of transition involved in its deexcitation are not known well. The gamma emission rates from this level to the ground and to the isomeric state have been measured. However, because of the low energies of the transitions the conversion coefficients are of great importance. An investigation of the effect of branching ratio of this level on the isomeric cross-section ratio may thus provide some valuable information on the type of transition involved. Based on the data given in Refs. [17–19] we calculated the branching ratios for different types of transition and the results are summarized in Table II. We performed nuclear model calculations assuming several variations in the branching ratios and the results are discussed below.

TABLE III. Measured cross sections and isomeric cross-section ratios of the ^{55}Mn(α,n)^{58}Co^{m,g} process. (σ_m was measured in this work; ($\sigma_m+\sigma_g$) values were taken from our earlier measurement [4].)

		^{55}Mn(α,n)^{58}Co^m		^{55}Mn(α,n)^{58}Co^{m,g}	
α-particle energy	Error in α-particle energy	σ	$\Delta\sigma$	$\sigma_m/(\sigma_m+\sigma_g)$	$\Delta[\sigma_m/(\sigma_m+\sigma_g)]$
(MeV)	(MeV)	(mb)	(mb)		
7.06	0.30	6.1	0.5	0.47	0.03
8.46	0.29	57	4	0.42	0.07
9.29	0.28	122	9	0.52	0.01
10.80	0.27	264	18	0.59	0.01
12.02	0.25	275	19	0.52	0.14
12.58	0.24	441	31	0.63	0.01
15.22	0.23	440	31	0.68	0.01
15.89	0.22	321	22	0.72	0.02
16.73	0.21	367	26	0.74	0.01
18.31	0.20	264	18	0.79	0.01
19.82	0.18	182	13	0.78	0.01
21.43	0.17	101	7	0.75	0.03
23.76	0.16	67	5	0.80	0.03
25.06	0.15	47	3	0.73	0.02

IV. RESULTS AND DISCUSSION

A. Alpha-particle-induced reaction on manganese

The measured cross sections for the ^{55}Mn(α,n)^{58}Co^m reaction and the isomeric cross-section ratios, $\sigma_m/(\sigma_m+\sigma_g)$, for the ^{55}Mn($\alpha,n$)^{58}Co^{m,g} process are given in Table III. For calculating the ratios, the ($\sigma_m+\sigma_g$) values reported earlier [4] were used. Figure 2 shows the measured σ_m values. Our experimental data are in good agreement with those given in Ref. [20]. The results of model calculations suggest that the shapes of experimental and theoretical excitation functions are similar. However, the magnitude of the calculated curve

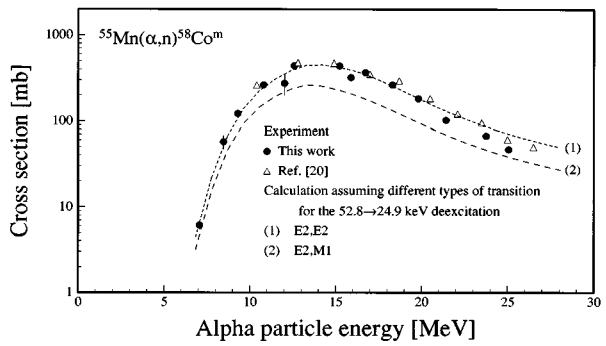

FIG. 2. Measured and calculated cross sections of the ^{55}Mn(α,n)^{58}Co^m reaction.

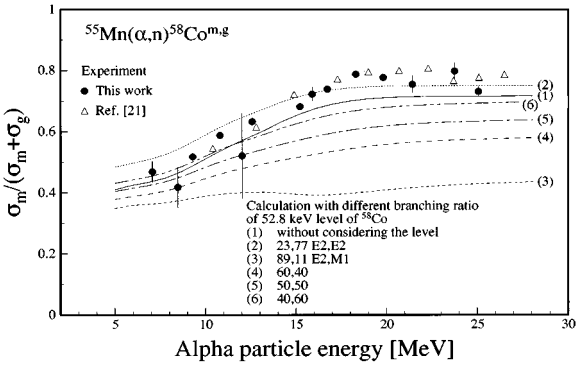

FIG. 3. Measured and calculated isomeric cross-section ratios of the ^{55}Mn$(\alpha,n)^{58}$Co^{m,g} reaction.

is significantly lower if the branching ratio of the 52.8 keV level is deduced assuming an $M1$ transition to the isomeric level at 24.9 keV.

The isomeric cross-section ratios are shown in Fig. 3. Our experimental data are in good agreement with those given in Ref. [21]. The results of model calculations are strongly influenced by the 52.8-keV level. A neglect of this level gives quite good results. The proposed $M1$ transition [16] to the isomeric level at 24.9 keV (in ratios varying between 11 and 60 %) gives increasingly deteriorating results. Using the branching ratio calculated from $E2$-type transition, the measured and calculated data show better agreement, though in the low energy region (below 15 MeV) the calculated values are slight overestimates.

B. Proton-induced reaction on iron

The measured cross sections for the ^{58}Fe$(p,n)^{58}$Co^{m} reaction and the isomeric cross-section ratios for the ^{58}Fe$(p,n)^{58}$Co^{m,g} process are summarized in Table IV. The latter were obtained from the σ_m data given here and the $(\sigma_m+\sigma_g)$ values reported earlier [4]. The data for the ^{58}Fe$(p,n)^{58}$Co^{m} reaction were deduced from measurements on ^{nat}Fe via normalization to 100% ^{58}Fe. The contribution of the ^{57}Fe$(p,\gamma)^{58}$Co^{m+g} process to the production of ^{58}Co^{m+g} seems to be negligible. Our measured data for ^{58}Fe$(p,n)^{58}$Co^{m+g} reaction in the energy range 3.1–4.9 MeV are in good agreement with the data given in Ref. [22] that were measured on 93.23% enriched ^{58}Fe target. Therefore the contribution of the (p,γ) process to our cross section is less than the error in our work (3 mb) at the lowest cross section value [4]. The model calculation shows that the (p,γ) cross section does not change more than by a factor of 2 in the investigated energy range. Thus the estimated contribution of the ^{57}Fe$(p,\gamma)^{58}$Co^{m+g} process to the ^{58}Fe$(p,n)^{58}$Co^{m+g} cross sections is less than 6 mb, that is 1–2 % at the higher energies. As far as we know, no data have been reported for this reaction in the literature. The experimental data are reproduced in Fig. 4 together with the results of model calculations using two types of branching of the 52.8→24.9 keV deexcitation. Obviously the $E2$-type transition leads to an overestimate of the cross section and the $M1$-type transition to an underestimate. The shapes of the calculated excitation functions are, however, in good agreement with the experimental one.

TABLE IV. Measured cross sections and isomeric cross-section ratios of ^{58}Fe$(p,n)^{58}$Co^{m,g} process. (σ_m was measured in this work; $(\sigma_m+\sigma_g)$ values were taken from our earlier measurement [4].)

		^{58}Fe$(p,n)^{58}$Co^{m}		^{58}Fe$(p,n)^{58}$Co^{m,g}	
Proton energy	Error in proton energy	σ	$\Delta\sigma$	$\sigma_m/(\sigma_m+\sigma_g)$	$\Delta[\sigma_m/(\sigma_m+\sigma_g)]$
(MeV)	(MeV)	(mb)	(mb)		
3.54	0.21	18	2		
4.90	0.20	34	3	0.21	0.02
5.71	0.23	82	7	0.24	0.04
6.48	0.22	110	9	0.24	0.02
7.16	0.19	151	12	0.29	0.03
7.48	0.21	167	14	0.32	0.03
8.13	0.20	183	16	0.29	0.03
8.02	0.18	171	14	0.31	0.04
8.74	0.19	224	18	0.34	0.03
8.81	0.17	209	17	0.36	0.03
9.32	0.18	218	19	0.40	0.06
10.17	0.16	258	21	0.39	0.04
10.11	0.17	256	21	0.34	0.05
10.63	0.16	265	22	0.32	0.05
10.84	0.15	294	23	0.41	0.04
10.98	0.19	254	21	0.40	0.05
11.14	0.15	280	23	0.38	0.06
11.21	0.19	289	24	0.39	0.04
11.63	0.18	269	24	0.38	0.04
11.86	0.18	289	24	0.38	0.03
12.46	0.17	266	23	0.39	0.04
12.48	0.17	291	23	0.41	0.04
13.53	0.16	232	21	0.41	0.04
13.55	0.16	233	20	0.43	0.04
14.09	0.15	225	18	0.46	0.04
14.12	0.15	211	19	0.46	0.04

The isomeric cross-section ratios for the ^{58}Fe$(p,n)^{58}$Co^{m,g} process are shown in Fig. 5. Without considering the 52.8 keV level the model calculation is in good

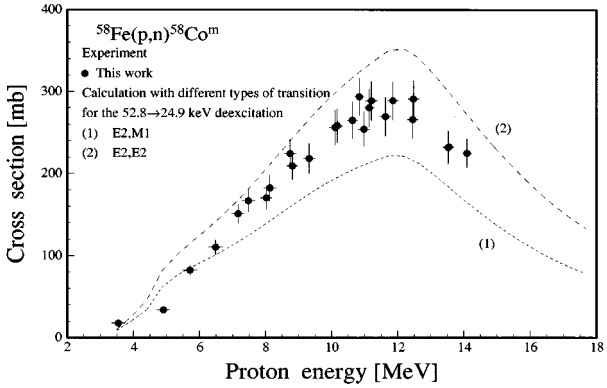

FIG. 4. Measured and calculated cross sections of the ^{58}Fe$(p,n)^{58}$Co^{m} reaction. The experimental data were deduced from measurements on ^{nat}Fe via normalization to 100% ^{58}Fe.

TABLE V. Measured cross sections and isomeric cross-section ratios of $^{nat}Fe(d,xn)^{58}Co^{m,g}$ process. (σ_m was measured in this work; ($\sigma_m+\sigma_g$) values were taken from our earlier measurement [4].)

Deuteron energy	Error in deuteron energy	$^{nat}Fe(d,xn)^{58}Co^{m}$ σ	$\Delta\sigma$	$^{nat}Fe(d,xn)^{58}Co^{m,g}$ $\sigma_m/(\sigma_m+\sigma_g)$	$\Delta[\sigma_m/(\sigma_m+\sigma_g)]$
(MeV)	(MeV)	(mb)	(mb)		
3.67	0.22	0.77	0.06	0.40	0.04
4.45	0.22	1.56	0.13	0.39	0.04
5.65	0.20	2.32	0.20	0.36	0.04
6.25	0.20	2.40	0.21		
7.23	0.19	2.36	0.20	0.36	0.04
7.38	0.22	2.85	0.21	0.44	0.04
7.74	0.19	2.61	0.21	0.39	0.04
7.83	0.20	2.73	0.20	0.41	0.04
8.26	0.20	2.72	0.21	0.45	0.04
8.51	0.18	2.46	0.22	0.40	0.04
9.05	0.18	2.23	0.20	0.36	0.04
9.06	0.20	2.53	0.19	0.44	0.04
9.48	0.18	2.55	0.19	0.47	0.04
9.85	0.18	2.50	0.19	0.45	0.04
10.16	0.17	2.25	0.22	0.41	0.05
10.23	0.17	2.26	0.21	0.40	0.05
10.56	0.18	2.45	0.18	0.47	0.04
10.94	0.16	2.31	0.17	0.45	0.04
11.28	0.16	2.26	0.17	0.46	0.04
11.33	0.16	2.04	0.20	0.40	0.05
11.57	0.16	2.35	0.18	0.49	0.04
11.62	0.16	2.14	0.21	0.43	0.05
12.29	0.15	2.17	0.16	0.47	0.05
12.60	0.15	2.22	0.17	0.46	0.04
12.70	0.15	2.16	0.21	0.44	0.05
12.85	0.15	2.33	0.17	0.50	0.04
12.97	0.15	2.08	0.20	0.44	0.05

agreement with the experimental data. The calculation overestimates the ratio while using $E2$-type transition for the 52.8→24.9 keV deexcitation but underestimates it by using $M1$-type transition.

A comparison of the measured isomeric cross-section ratios of $^{58}Fe(p,n)^{58}Co^{m,g}$ and $^{55}Mn(\alpha,n)^{58}Co^{m,g}$ processes shows (cf. Figs. 5 and 3, respectively) that the values for the former reaction are much lower than those for the latter reaction. The energy dependence of the ratio is also somewhat different: in the case of proton-induced reaction it shows a monotonous increase with energy whereas for the α-particle-induced reaction it increases initially, reaching a maximum value at about 17 MeV and is thereafter almost energy independent. The model calculations support these energy dependences. The difference between the results of the two calculations ($E2$- or $M1$-type transition for the 52.8→24.9 keV deexcitation) for the proton-induced reaction is, however, much smaller than that in the case of the α-particle-induced reaction.

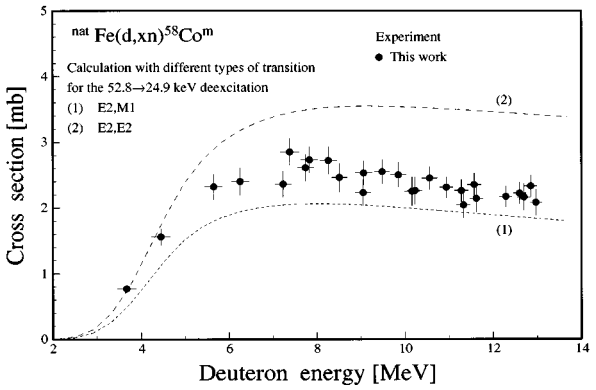

FIG. 6. Measured and calculated cross sections of the $^{nat}Fe(d,xn)^{58}Co^{m}$ process.

C. Deuteron-induced reaction on iron

The measured cross sections for the $^{nat}Fe(d,xn)^{58}Co^{m}$ reaction and the isomeric cross-section ratios for the $^{nat}Fe(d,xn)^{58}Co^{m,g}$ process are given in Table V. The isomeric cross-section ratios were obtained from the σ_m data given here and the ($\sigma_m+\sigma_g$) values reported earlier [4]. As far as we know, no other data have been reported for this reaction in the literature. The data refer to ^{nat}Fe since several reactions like $^{56}Fe(d,\gamma)$, $^{57}Fe(d,n)$, and $^{58}Fe(d,2n)$ can contribute. In general, however, the major contribution is expected to stem from the $^{57}Fe(d,n)$ reaction since over the investigated energy range the cross section of the

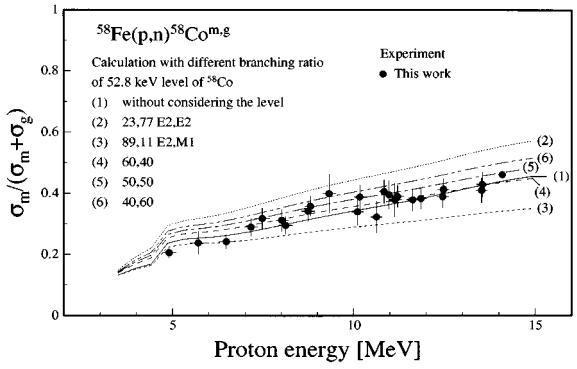

FIG. 5. Measured and calculated isomeric cross-section ratios of the $^{58}Fe(p,n)^{58}Co^{m,g}$ reaction.

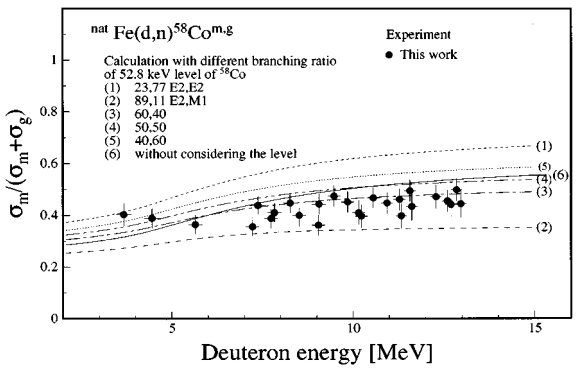

FIG. 7. Measured and calculated isomeric cross-section ratios of the $^{nat}Fe(d,xn)^{58}Co^{m,g}$ process.

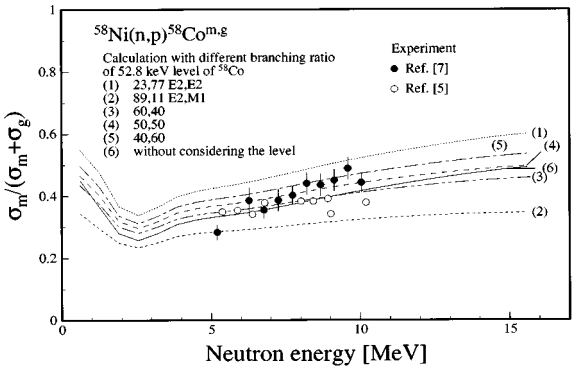

FIG. 8. Measured and calculated isomeric cross-section ratios of the ^{58}Ni$(n,p)^{58}$Co^{m,g} reaction.

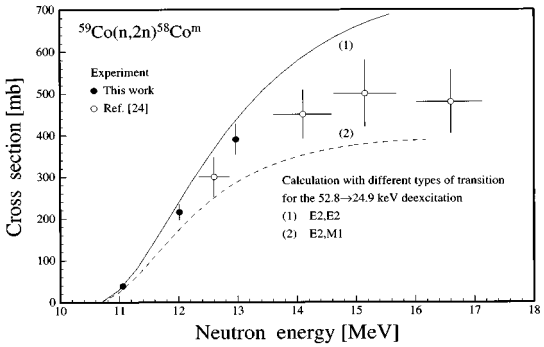

FIG. 9. Measured and calculated cross sections of the ^{59}Co$(n,2n)^{58}$Co^{m} process.

^{56}Fe(d,γ) process should be small and the contribution of the ^{58}Fe$(d,2n)$ process low because of its much lower isotopic abundance.

The measured and calculated excitation functions for the $^{\text{nat}}$Fe$(d,xn)^{58}$Co^{m} reaction are shown in Fig. 6. In the model calculation due consideration was given to the fact that the deuteron-induced reaction can be described only if a reduction factor is used in the input channel. This reduction factor takes into account the contribution of the direct reactions which is not included in the used model (cf. Ref. [4]). We applied the same reduction factor ($R=0.56$) as used in the description of the $^{\text{nat}}$Fe$(d,xn)^{58}$Co^{m+g} process (cf. Ref. [4]). Similar to the proton-induced reaction (see above), the shapes of the calculated excitation functions are in good agreement with the experimental one. Again the use of $E2$- or $M1$-type transition for the 52.8→24.9 keV deexcitation leads to different results.

Figure 7 shows the experimental isomeric cross-section ratios as well as the results of the model calculations. The experimental values are almost constant or show a slight increase with increasing deuteron energy. The model calculation using $M1$-type transition for the 52.8→24.9 keV deexcitation gives lower values of the isomeric cross-section ratio than the experimental one, while use of $E2$-type transition overestimates the ratio. This overestimation is much more than in the case of proton-induced reaction. Without considering the 52.8 keV level the theoretical results are nearer to the experimental data.

TABLE VI. Measured cross sections and isomeric cross-section ratios of ^{59}Co$(n,2n)^{58}$Co^{m,g} process. (σ_m was measured in this work; ($\sigma_m+\sigma_g$) values were taken from earlier measurements [2,23].)

Neutron energy	Error in neutron energy	^{59}Co$(n,2n)^{58}$Co^{m} σ	$\Delta\sigma$	^{59}Co$(n,2n)^{58}$Co^{m,g} $\sigma_m/(\sigma_m+\sigma_g)$	$\Delta[\sigma_m/(\sigma_m+\sigma_g)]$
(MeV)	(MeV)	(mb)	(mb)		
11.06	0.15	39	4	0.80	0.16
12.01	0.15	216	20	0.68	0.07
12.97	0.15	390	37	0.75	0.06

D. Neutron-induced reactions

Figure 8 shows the isomeric cross-section ratio of the ^{58}Ni$(n,p)^{58}$Co^{m,g} process as a function of the neutron energy. The values were obtained from the experimental σ_m data reported by us earlier [7] and the ($\sigma_m+\sigma_g$) values given in the literature (cf. Ref. [2]). Comparing the experimental data of ^{58}Ni$(n,p)^{58}$Co^{m,g} and ^{55}Mn$(\alpha,n)^{58}$Co^{m,g} reactions one finds that the isomer ratio in the former reaction is much lower than that in the latter reaction. The energy dependences of the ratios also show different characters.

Nuclear model calculations on the ^{58}Ni$(n,p)^{58}$Co^{m,g} process were also done assuming both the $M1$- and $E2$-type transitions for the 52.8→24.9 keV deexcitation. The results given in Fig. 8 show that the $M1$-type transition yields lower values of the isomeric cross-section ratio than the experimental one, while the calculation with $E2$-type transition overestimates the data. Without considering the 52.8-keV level the model calculation is nearer to the experimental data, though resulting in a slight underestimation of the data.

The measured cross sections for the ^{59}Co$(n,2n)^{58}$Co^{m} reaction and the isomeric cross-section ratios for the ^{59}Co$(n,2n)^{58}$Co^{m,g} process are summarized in Table VI. For the ^{59}Co$(n,2n)^{58}$Co^{m+g} process a large number of measurements have been performed (cf. Ref. [2]), and more recently a new measurement near the threshold has been described [23]. We made use of those data.

Our experimental data for the ^{59}Co$(n,2n)^{58}$Co^{m} reaction are reproduced in Fig. 9 together with the literature values [24]. The agreement appears to be good. The results of

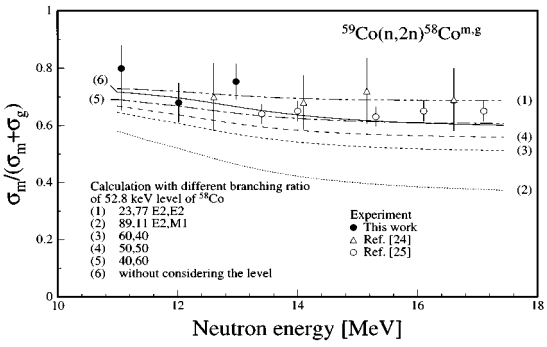

FIG. 10. Measured and calculated isomeric cross-section ratios of the ^{59}Co$(n,2n)^{58}$Co^{m,g} process.

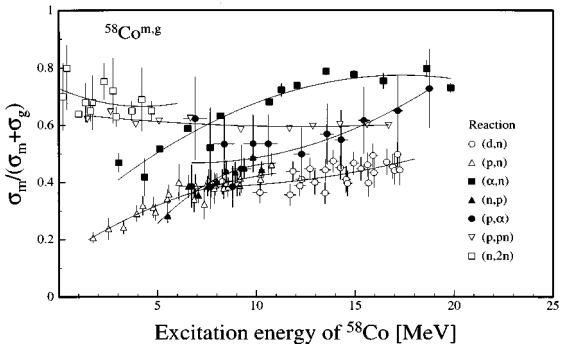

FIG. 11. Measured isomeric cross-section ratios for different charged particle and neutron-induced reactions plotted as a function of the maximum excitation energy of the product nucleus ^{58}Co. The curves give eye guides to the data on each reaction.

model calculations using two types of branching of the 52.8→24.9 keV deexcitation are also given. The $E2$-type transition gives better estimation of the cross section than the $M1$-type transition. The shapes of the calculated excitation functions are, however, in good agreement with the experimental one. The experimental data for the ^{59}Co$(n,2n)^{58}$Co^{m+g} reaction described in the literature were found to be in good agreement with the results of our model calculations.

The isomeric cross-section ratios for the ^{59}Co$(n,2n)^{58}$Co^{m,g} process are given in Fig. 10. In addition to our own data, some values reported in the literature [24,25] are also shown. In general, there appears to be a good agreement. Without considering the 52.8-keV level, the result of model calculation agrees with the experimental data.

E. Isomeric cross-section ratio in various reaction channels

The measured isomeric cross-section ratios for the abovementioned five processes studied in this work, viz. ^{55}Mn(α,n), ^{58}Fe(p,n), $^{\text{nat}}$Fe(d,xn), ^{58}Ni(n,p), and ^{59}Co$(n,2n)$, as well as for the ^{61}Ni(p,α) [3] and ^{59}Co(p,pn) [6] reactions reported in the literature are shown in Fig. 11 as a function of the maximum excitation energy of the product nucleus ^{58}Co. The values show large differences, depending on the type of the reaction. The (p,n), (d,n), and (α,n) reactions proceed through the same compound nucleus (^{59}Co). In (p,pn) and $(n,2n)$ reactions, although the compound nucleus formed is different, the emission of the first nucleon leads to the formation of the intermediate excited nucleus ^{59}Co. The emission of the second nucleon, which governs the isomeric ratio, is thus again from the excited nucleus ^{59}Co. The large differences in the ratios therefore possibly arise from the different angular momentum distribution of the produced compound nucleus (the contribution of the precompound reaction being not very important in the investigated energy range).

In general, the isomeric cross-section ratio is expected to depend on several factors, such as spin of the target nucleus, type, and energy of the projectile used, type of the emitted particle, and, more importantly, on the spins of the isomeric states concerned. Since in Fig. 11 the results apply to the same product isomeric pair, a possible explanation for the trends is to be sought in the first three factors involved. The spin of the target nucleus seems to play an important role. The highest isomeric cross-section ratios are observed in the case of ^{59}Co$(n,2n)$, ^{59}Co(p,pn), ^{55}Mn(α,n), and ^{61}Ni(p,α) processes. The spins of the target nuclei concerned, viz. ^{59}Co, ^{55}Mn, and ^{61}Ni, are $7/2^-$, $5/2^-$, and $3/2^-$, respectively. The isomer ratios for ^{58}Fe(p,n), $^{\text{nat}}$Fe(d,xn), and ^{58}Ni(n,p) reactions are relatively low, and the spins of the respective target nuclei, ^{58}Fe, ^{57}Fe, and ^{58}Ni, are also low (0^+, $1/2^-$, 0^+, respectively). The somewhat lower and constant values of the ratio in proton- and neutron-induced reactions on the high-spin target nucleus ^{59}Co, in comparison to (p,α) and (α,n) reactions at higher excitation energies, may be attributed to the occurrence of a two-step process.

The effect of reaction channel may be manifested through a change in the projectile or the emitted particle. Figure 11 suggests that the α-particle-induced reaction leads to somewhat higher isomer ratio, especially with increasing excitation energy (cf. also Ref. [14]); but at lower excitation energies the isomer ratios for (p,pn) and $(n,2n)$ reactions are higher than that in the α-particle-induced reaction. The high isomer ratio for the (α,n) process may be caused by the high kinetic energy of the α-particle involved, thereby allowing the absorption of the particle with high angular momentum. The effect of the α particle in the exit channel, however, is not very significant. This agrees with our recent observation on a few other isomeric pairs (cf. Refs. [10,26]). Obviously, for a better understanding of the effect of reaction channel, more investigations are needed.

V. CONCLUSIONS

For the five reactions investigated in this work, viz. ^{55}Mn(α,n), ^{58}Fe(p,n), $^{\text{nat}}$Fe(d,xn), ^{58}Ni(n,p), and ^{59}Co$(n,2n)$, the results of nuclear model calculations on the isomeric cross-section ratio of the isomeric pair ^{58}Co^{m,g} are very strongly dependent on the assumed type of transition for the 52.8→24.9 keV deexcitation. It is not possible to find a branching ratio which would fit all the calculated isomeric cross-section ratios to the experimental data. In general, it is concluded that the model calculations can describe the measured isomeric cross-section ratios of charged particle as well as neutron-induced reactions well, provided the level scheme of the product nucleus and the branching ratios of the various levels are adequately known (cf. also Refs. [14,15]).

The experimental isomeric cross-section ratio depends on the type of reaction involved and seems to be related to the angular-momentum distribution of the compound nucleus. The spin of the target nucleus and the energy of the incident particle play an important role. The isomeric cross-section ratio was found to be relatively high for target nuclei with high-spin values.

ACKNOWLEDGMENTS

We thank Professor G. Stöcklin and Professor J. Csikai for their active support of this program. This work was done under a German-Hungarian bilateral agreement [Nos. 13(X237.1) and 231.7] and it was partly supported by the Hungarian National Science Foundation (OTKA 1734/91 and OTKA T016713).

[1] *Table of Isotopes*, edited by C. M. Lederer and V. S. Shirley (Wiley, New York, 1978); E. Browne and R. B. Firestone, in *Table of Radioactive Isotopes*, edited by V. S. Shirley (Wiley, New York, 1986).

[2] V. McLane, C. L. Dunford, and P. F. Rose, *Neutron Cross Sections* (Academic, New York, 1988), Vol. 2.

[3] S. Sudár, F. Szelecsényi, and S. M. Qaim, Phys. Rev. C **48**, 3115 (1993).

[4] S. Sudár and S. M. Qaim, Phys. Rev. C **50**, 2408 (1994).

[5] Cs. M. Buczkó, J. Csikai, S. Sudár, Á. Grallert, S. A. Jonah, B. W. Jimba, T. Chimoye, and M. Wagner, Phys. Rev. C **52**, 1940 (1995).

[6] J. W. Meadows, R. M. Diamond, and R. A. Sharp, Phys. Rev. **102**, 190 (1956).

[7] S. Sudár, J. Csikai, S. M. Qaim, and G. Stöcklin, in *Proceedings of the International Conference on Nuclear Data for Science and Technology*, Jülich, 1991, edited by S. M. Qaim (Springer-Verlag, Berlin, 1992), p. 291.

[8] S. M. Qaim, in *Proceedings of the International Conference on Nuclear Data for Science and Technology*, Gatlinburg, 1994, edited by J. K. Dickens (American Nuclear Society, Inc., LaGrange Park, 1994), p. 186.

[9] S. M. Qaim, R. Wölfle, M. M. Rahman, and H. Ollig, Nucl. Sci. Eng. **88**, 143 (1984).

[10] F. Cserpák, S. Sudár, J. Csikai, and S. M. Qaim, Phys. Rev. C **49**, 1525 (1994).

[11] I. Birn, NEUT, Ein Programm zur Berechnung von Neutronenspektren erzeugt durch die $D(d,n)^3$He-Reaktion in einem Gastarget am Zyklotron, KFA Jülich, Internal Report INC-IB-1, 1992.

[12] IRDF (International Radiation Dosimetry File, 1990), issued by the International Atomic Energy Agency, Vienna, as a computer file.

[13] M. Uhl and B. Strohmaier, Computer Code for Particle Induced Activation Cross Section and Related Quantities, Institut für Radiumforschung und Kernphysik Report 76/01, 1976, and addenda to this report. See also B. Strohmaier and M. Uhl, International Atomic Energy Agency Report IAEA-SMR-43, 1980, p. 313.

[14] S. M. Qaim, A. Mushtaq, and M. Uhl, Phys. Rev. C **38**, 645 (1988).

[15] N. I. Molla, S. M. Qaim, and M. Uhl, Phys. Rev. C **42**, 1540 (1990).

[16] L. K. Peker, Nucl. Data Sheets **42**, 457 (1984); R. L. Auble, *ibid*. **20**, 253 (1977); T. W. Burrows and M. R. Bhat, *ibid*. **47**, 1 (1986); P. Anderson, L. P. Ekström, and J. Lyttkens, *ibid*. **39**, 641 (1983); H. Verhuel and R. L. Auble, *ibid*. **23**, 455 (1978).

[17] B. Haas, C. Gehringer, J. Chavalier, J. C. Merdinger, and E. Bozek, Nucl. Phys. **A194**, 249 (1972).

[18] R. G. H. Robertson and R. G. Summers-Gill, Can. J. Phys. **49**, 1186 (1971).

[19] R. S. Hager and C. Seltzer, Nucl. Data **4**, 1 (1968).

[20] Long Xianguan, He Fuqing, Peng Xiufen, and Liu Mantian, High Energy Phys. Nucl. Phys. **14**, 443 (1990).

[21] Long Xianguan, He Fuqing, Peng Xiufen, and Liu Mantian, Chin. J. Nucl. Phys. **11**, 25 (1989).

[22] S. G. Tims, A. F. Scott, A. J. Morton, V. Y. Hansper, and D. G. Sargood, Nucl. Phys. **A563**, 473 (1993).

[23] W. Mannhart, D. Schmidt, and Xia Haihong, in *Proceedings of the International Conference on Nuclear Data for Science and Technology* [8], p. 285.

[24] M. Bormann, F. Dreyer, U. Seebeck, and W. Voigts, Z. Naturforsch. **21a**, 988 (1966).

[25] S. K. Ghorai, J. E. Gaiser, and W. L. Alford, Ann. Nucl. Energy **7**, 41 (1980).

[26] I.-G. Birn, B. Strohmaier, H. Freiesleben, and S. M. Qaim, Phys. Rev. C **52**, 2546 (1995).